Delft University of Technology

Range equation for hybrid-electric aircraft with constant power split

De Vries, Reynard; Hoogreef, Maurice F.M.; Vos, Roelof

Important note
To cite this publication, please use the final published version (if applicable).
Please check the document version above.

Engineering Notes

Range Equation for Hybrid-Electric Aircraft with Constant Power Split

Reynard de Vries,* Maurice F. M. Hoogreef,† and Roelof Vos‡
Delft University of Technology, 2629 HS Delft, The Netherlands

https://doi.org/10.2514/1.C035734

Nomenclature

a, b, c, m, n	=	dummy variables
D	=	drag, N
E	=	energy, J
e	=	specific energy, J/kg
g	=	gravitational acceleration, m/s^2
L	=	lift, N
P	=	power, W
R	=	range, m
T	=	thrust, N
t	=	time, s
V	=	velocity, m/s
W	=	weight, N
γ	=	flight path angle, rad
η	=	conversion or transmission efficiency
Φ	=	supplied power ratio

Subscripts

bat	=	battery
eg	=	electrical generator
em	=	electrical motor
end	=	end of mission segment
f	=	fuel
gt	=	gas turbine or thermal engine
OE	=	operating empty
PL	=	payload
p	=	propulsive
start	=	start of mission segment
TO	=	takeoff
tot	=	total
0	=	start of mission
1, 2, 3	=	powertrain branch indices

I. Introduction

THERE has been a surge in research related to hybrid-/ electric propulsion (HEP) over the past decade, since this technology

*Ph.D. Candidate, Faculty of Aerospace Engineering; r.devries@tudelft.nl. Member AIAA.

†Assistant Professor, Faculty of Aerospace Engineering; m.f.m.hoogreef@tudelft.nl. Member AIAA.

‡Assistant Professor, Faculty of Aerospace Engineering; r.vos@tudelft.nl. Associate Fellow AIAA.

has the potential to reduce the energy consumption and in-flight emissions of commercial aircraft and, therefore, to bring the aviation sector closer to the sustainability targets established by the European Commission [1] and NASA [2]. Previous studies have shown that hybrid-electric [3,4] and fully-electric [5] general-aviation aircraft can lead to a reduction in both emissions and operating costs for short ranges, when compared with fuel-based alternatives. However, due to the enormous energy and power requirements of large passenger aircraft, fully battery-based propulsion is not a viable option to substantially reduce the climate impact of the aviation sector as a whole [6], unless the mission range is significantly reduced, or unrealistically high battery energy densities are assumed [7]. For this reason, hybrid architectures (especially parallel [8–10] and turbo-electric [11–14] ones) are often investigated as a potential solution for large passenger aircraft.

For a fair comparison of these different configurations, simplified design-space exploration [15] or sizing [16–20] methods that are explicitly developed for HEP aircraft must be used. Although only some of these sizing methods are generic enough to directly compare different powertrain architectures, the amount of energy required to complete a predefined mission has to be computed in all of them. In most design studies, this is done by means of a time-stepping mission analysis [4,18–24]. However, this already requires information regarding the aircraft layout and power-control strategy, which may not be available at the very beginning of a clean-sheet design process. In that case, a more simplified approach can be used to estimate the energy consumption. For conventional aircraft, this is typically done in the class I sizing phase by means of the well-established Breguet range equation (see, e.g., Refs. [25–27]), which can be expressed as

$$R = \eta_{\mathrm{gt}}\eta_{\mathrm{p}}\left(\frac{L}{D}\right)\left(\frac{e_{\mathrm{f}}}{g}\right)\ell_{\mathrm{n}}\left(\frac{W_{\mathrm{OE}} + W_{\mathrm{PL}} + W_{\mathrm{f}}}{W_{\mathrm{OE}} + W_{\mathrm{PL}}}\right) \qquad (1)$$

where $W_{\mathrm{OE}} + W_{\mathrm{PL}} + W_{\mathrm{f}}$ equals the takeoff weight of the aircraft, W_{TO}. This equation shows that the range depends on the weight breakdown of the aircraft, the specific energy of the fuel used, and the propulsive efficiency η_{p}, aerodynamic efficiency L/D, and combustion-engine efficiency η_{gt} of the aircraft. There is a logarithmic dependency of range on fuel weight, because the fuel weight (and thus the aircraft weight) decreases throughout the mission.

A range equation can also be derived for fully-electric aircraft in a similar fashion. In that case, the equation is simplified further, because the mass of the energy source (batteries) remains constant throughout the mission. Numerous studies (see, e.g., Refs. [28–34]) have already shown that, in this case, the range equation is given by

$$R = \eta_{\mathrm{em}}\eta_{\mathrm{p}}\left(\frac{L}{D}\right)\left(\frac{e_{\mathrm{bat}}}{g}\right)\left(\frac{W_{\mathrm{bat}}}{W_{\mathrm{OE}} + W_{\mathrm{PL}} + W_{\mathrm{bat}}}\right) \qquad (2)$$

Here, the efficiency factor η_{em} comprises the efficiencies of all electrical components connected in series between the energy source (batteries) and the propulsor shaft. Because the aircraft weight remains constant, there is no logarithmic dependency, and the range is directly proportional to the battery weight fraction $W_{\mathrm{bat}}/W_{\mathrm{TO}}$ instead.

Multiple authors have also derived range equations for hybrid-electric aircraft, which combine the two energy sources. However, the formulations encountered in literature are based on inaccurate assumptions or are limited to a specific powertrain architecture and control strategy. For example, several studies directly add up the contribution of the consumable energy source [Eq. (1)] and the non-consumable energy source [Eq. (2)] to compute the total range [3,35,36]. This is, however, incorrect, because Eq. (2) is only valid

when the weight of the aircraft remains constant, which is not the case for hybrid-electric aircraft. Nam [37] derived a range equation valid for powertrains with a single energy source, which can be consumable or non-consumable. Although the formulation of Nam could account for hybrid-electric systems with constant power split if an "equivalent" single energy source is defined, the equation itself is not directly applicable without significant manipulation. Voskuijl et al. [22] do not make the distinction between the battery energy available and the installed battery energy capacity—the latter of which determines battery weight—thus leading to erroneous results when integrating the energy consumption along the mission.[§] Ravishankar and Chakravarthy [38] assume that the fuel mass-flow rate is constant throughout the mission, thus obtaining a series of expressions that do not present the logarithmic dependency reflected in Eq. (1). The formulation presented by Rohacs and Rohacs [39], to the contrary, maintains the logarithm in the limit case of a fully-electric aircraft, which is inconsistent with Eq. (2). Finally, Elmousadik et al. [40] implicitly assume that first all fuel is burnt, and afterward all battery energy is consumed. One could argue that this leads to the maximum range for a given aircraft weight breakdown, because the aircraft weight is reduced as much as possible at the beginning, and kept at a minimum for the rest of the mission. However, this implies that both the thermal engine and the electrical components must be sized to be able to provide 100% of the required propulsive power, thus leading to a significant increase in the empty-weight fraction of the aircraft. This highlights the interconnected nature of the sizing process, especially for hybrid-electric aircraft.

The objective of this Engineering Note is therefore to derive a simple range equation valid for aircraft with a generic hybrid-electric powertrain architecture. In this process, it becomes evident that conventional fuel-based configurations and fully-electric configurations are actually limit cases of the hybrid-electric powertrain. To obtain a closed form of the range equation, a constant power split throughout the mission is assumed. In practice, it is unlikely that a constant power split will lead to the best design, and therefore it is important to analyze variable power-split strategies early in the design process, as indicated by several authors [19,41]. Nevertheless, a simplified range equation can be applied to discrete mission segments with constant power split, or to determine initial values for more advanced design methods. Moreover, the derivation and application of the range equation helps to understand the influence of some of the key parameters and design considerations involved in the sizing process of hybrid-electric aircraft.

II. Simplified Powertrain Representation

The simplified schematic representation of the different powertrain architectures used in this study is based on the classification of Refs. [19,42]. When considering hybrid-electric powertrain architectures with only one type of propulsion system, one can distinguish between powertrains with a mechanical node (a gearbox), and powertrains with an electrical node (a power management and distribution system). Parallel and serial powertrains are examples of such architectures, as shown in Figs. 1a and 1b, respectively. Conventional, turboelectric, and fully electric powertrains, on the other hand, can be identified as simplified versions of these two architectures.

At this point the simplification is made that no power losses exist at the nodes. In this case, the two powertrain types can be further simplified and merged into a single schematic, shown in Fig. 1c. This generic representation presents two energy sources (fuel and batteries) and one energy sink (the ambient air). The three branches that connect the node with the energy sources and sinks are labeled "1," "2," and "3" for simplicity. Each branch is modeled by a single constant transmission efficiency η, which encompasses different elements depending on the powertrain architecture. The relation between each branch and the different architectures is summarized in Table 1.

a) **Mechanical node (parallel architecture)**

b) **Electrical node (serial architecture)**
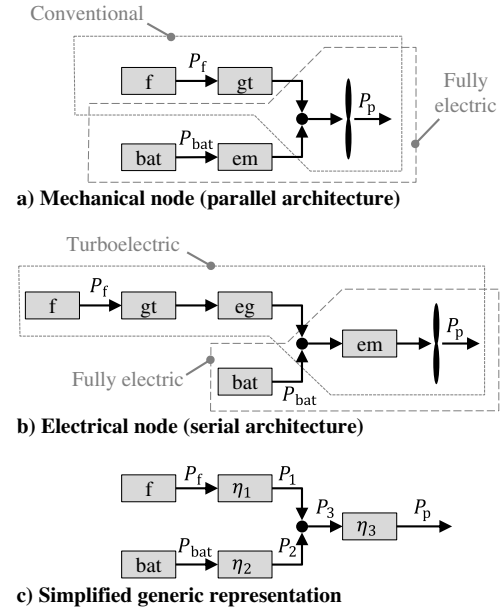

c) **Simplified generic representation**

Fig. 1 Simplified schematic representations of powertrain architectures.

Finally, a power-split parameter is required to define how the power coming from the two energy sources is shared at the node. For this, the supplied power ratio [19,43] is used:

$$\Phi = \frac{P_{\mathrm{bat}}}{P_{\mathrm{bat}} + P_{\mathrm{f}}} \tag{3}$$

The supplied power ratio is assumed to be constant in the present analysis, as discussed in the Introduction. Equation (3) can be rewritten as

$$P_{\mathrm{bat}} = \frac{\Phi}{1 - \Phi} P_{\mathrm{f}} \tag{4}$$

where, in an intermediate step, both sides of the equation have been divided by the term $(1 - \Phi)$. This will lead to a singularity for $\Phi = 1$, as discussed in Sec. IV.

III. Derivation of the Hybrid Electric Range Equation

The derivation starts by considering the power balance at the node of the powertrain, $P_3 = P_1 + P_2$, which can be written as

$$\frac{P_{\mathrm{p}}}{\eta_3} = \eta_1 P_{\mathrm{f}} + \eta_2 P_{\mathrm{bat}} \tag{5}$$

The powers included on the right-hand side of Eq. (5) are defined as positive when the energy sources are being depleted, such that

$$P_{\mathrm{f}} = -\frac{\mathrm{d}E_{\mathrm{f}}}{\mathrm{d}t} \tag{6a}$$

Table 1 Relation between powertrain branch efficiencies and component efficiencies for powertrains with mechanical (conventional, parallel, or fully-electric architectures) and electrical (turboelectric, serial, or fully-electric architectures) nodes

Simplified representation	Mechanical-node architectures	Electrical-node architectures
$\eta_1 =$	η_{gt}	$\eta_{\mathrm{gt}}\eta_{\mathrm{eg}}$
$\eta_2 =$	η_{em}	1
$\eta_3 =$	η_p	$\eta_{\mathrm{em}}\eta_p$

$$P_{\text{bat}} = -\frac{dE_{\text{bat}}}{dt} \tag{6b}$$

The propulsive power included on the left-hand side of Eq. (5) can be related to the thrust required in the current flight condition, since $P_p = T \cdot V$. To this end, Fig. 2 indicates the main forces acting on the aircraft in steady symmetric flight. The thrust vector is assumed to be aligned with the velocity vector, and the aircraft is assumed to fly at a constant lift coefficient and velocity, such that the lift-to-drag ratio is maintained. Given that the weight of the aircraft decreases over time, the altitude of the aircraft will increase. However, the resulting flight path angle γ is approximately zero, and thus quasi-level flight is assumed. Under these conditions, the propulsive power can be expressed as

$$P_p = \frac{W \cdot V}{(L/D)} \tag{7}$$

By inserting Eqs. (4), (6), and (7) into Eq. (5) and reorganizing terms, one obtains

$$V = -\eta_3 \left(\frac{L}{D}\right) \frac{1}{W} \frac{dE_f}{dt} \left(\eta_1 + \eta_2 \frac{\Phi}{1-\Phi}\right) \tag{8}$$

Because the flight speed is constant, the left-hand side of Eq. (8) can be integrated to obtain the range covered during a mission segment that starts at a generic time instance t_{start} and ends at t_{end}:

$$\int_{t_{\text{start}}}^{t_{\text{end}}} V \, dt = R \tag{9}$$

Equation (8) can therefore be rewritten as

$$R = \eta_3 \left(\frac{L}{D}\right) \left(\eta_1 + \eta_2 \frac{\Phi}{1-\Phi}\right) \int_{t_{\text{end}}}^{t_{\text{start}}} \frac{1}{W(t)} \frac{dE_f}{dt} \, dt \tag{10}$$

where the integral limits have been swapped to remove the minus sign. The aircraft weight varies over time, since

$$W(t) = W_{\text{OE}} + W_{\text{PL}} + W_{\text{bat}} + W_f(t) \tag{11}$$

Note that the battery weight W_{bat} is not considered part of the operating empty weight. When relating battery and fuel weight to battery and fuel energy, it is important to make a distinction between the total energy capacity of the aircraft, and the remaining energy at a given point along the mission. Whereas the former is equal to the amount of energy available at the beginning of the mission, the latter varies over time. With this in mind, the two weight components can be expressed as

$$W_f(t) = \frac{g}{e_f} E_f(t) \tag{12a}$$

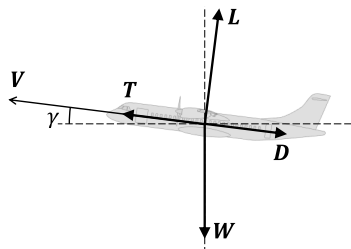$$W_{\text{bat}} = \frac{g}{e_{\text{bat}}} E_{0,\text{bat}} \tag{12b}$$

Fig. 2   Simplified free-body diagram of the aircraft.

In Eq. (12b), e_{bat} refers to the specific energy of the battery at pack level when it is fully charged, which is constant and known a priori. This value should include a weight penalty of the order of 20% [44] to ensure a minimum state-of-charge during the mission and avoid detrimental effects on battery life.

Subsequently, by inserting Eqs. (11), (12a), and (12b) into Eq. (10), the following expression is obtained:

$$R = \eta_3 \left(\frac{L}{D}\right) \left(\eta_1 + \eta_2 \frac{\Phi}{1-\Phi}\right)$$
$$\times \int_{t_{\text{end}}}^{t_{\text{start}}} \left(\frac{(dE_f/dt)}{W_{\text{OE}} + W_{\text{PL}} + (g/e_{\text{bat}})E_{0,\text{bat}} + (g/e_f)E_f(t)}\right) dt \tag{13}$$

The integral can be solved by recalling that $d(\ln(x))/dt = (1/x) \cdot dx/dt$, such that

$$R = \eta_3 \left(\frac{L}{D}\right) \left(\eta_1 + \eta_2 \frac{\Phi}{1-\Phi}\right)$$
$$\times \int_{t_{\text{end}}}^{t_{\text{start}}} \frac{e_f}{g} \frac{d}{dt} \left(\ln\left(W_{\text{OE}} + W_{\text{PL}} + \frac{g}{e_{\text{bat}}}E_{0,\text{bat}} + \frac{g}{e_f}E_f(t)\right)\right) dt \tag{14}$$

which, by evaluating the integral limits, leads to

$$R = \eta_3 \frac{e_f}{g} \left(\frac{L}{D}\right) \left(\eta_1 + \eta_2 \frac{\Phi}{1-\Phi}\right)$$
$$\times \ln\left[\frac{W_{\text{OE}} + W_{\text{PL}} + (g/e_{\text{bat}})E_{0,\text{bat}} + (g/e_f)E_f(t_{\text{start}})}{W_{\text{OE}} + W_{\text{PL}} + (g/e_{\text{bat}})E_{0,\text{bat}} + (g/e_f)E_f(t_{\text{end}})}\right] \tag{15}$$

Eq. (15) can be used to determine the range of a discrete mission segment if the fuel energy E_f or fuel weight W_f [see Eq. (12a)] at the beginning and end of the segment is known. This allows an evaluation of different mission phases with different power splits or lift-to-drag ratios (e.g., cruise and diversion).

If all fuel is consumed, then $E_f(t_{\text{start}}) = E_{0,f}$ and $E_f(t_{\text{end}}) = 0$. Moreover, the fuel and battery energy carried on-board at the start of the mission can be related to the total energy $E_{0,\text{tot}} = E_{0,f} + E_{0,\text{bat}}$ by combining Eqs. (6a) and (6b) with Eq. (3) and integrating them over time, obtaining

$$E_{0,f} = (1 - \Phi)E_{0,\text{tot}} \tag{16a}$$

$$E_{0,\text{bat}} = \Phi E_{0,\text{tot}} \tag{16b}$$

Eq. (16a) and (16b) show that, because the supplied power ratio is constant throughout the mission, it is identical to the degree-of-hybridization of energy of the aircraft. Equation (15) is therefore reduced to

$$R = \eta_3 \frac{e_f}{g} \left(\frac{L}{D}\right) \left(\eta_1 + \eta_2 \frac{\Phi}{1-\Phi}\right)$$
$$\times \ln\left[\frac{W_{\text{OE}} + W_{\text{PL}} + (g/e_{\text{bat}})E_{0,\text{tot}}(\Phi + (e_{\text{bat}}/e_f)(1-\Phi))}{W_{\text{OE}} + W_{\text{PL}} + (g/e_{\text{bat}})\Phi E_{0,\text{tot}}}\right] \tag{17}$$

The range equation given by Eq. (17) is valid for conventional, serial, parallel, turboelectric, and fully-electric aircraft, as long as the supplied power ratio, flight speed, lift-to-drag ratio, and transmission efficiencies are constant. Note that the weight and energy components are expressed in their respective units to make the derivation easier to follow; however, when analyzing the range equation for different aircraft, the use of normalized variables such as weight fractions or energy fractions is recommended. Moreover, although Eq. (17) is straightforward to apply, it should be used with some caution. For example, it can be used to compute the total energy required for a given harmonic range only if most of the energy is

consumed in the cruise phase, for example, for long-haul flights. If not, Eq. (15) should be used instead to compute the energy requirements of specific mission segments. However, both formulations are inaccurate for climb and descent phases, because they assume a small flight-path angle ($\gamma \ll 1$). Furthermore, given that hybrid-electric configurations typically have much higher empty-weight fractions than conventional fuel-based aircraft (due to the increased powertrain weight [19,44,45]), it is important to assume appropriate empty-weight values when comparing different aircraft configurations.

IV.   Limit Cases

A.   Fully Fuel-Based Configurations

For fully fuel-based configurations, the supplied power ratio is equal to zero ($\Phi = 0$). Thus, Eq. (17) is reduced to

$$R = \eta_1 \eta_3 \frac{e_f}{g} \left(\frac{L}{D}\right) \ln\left(\frac{W_{OE} + W_{PL} + (g/e_f)E_{0,tot}}{W_{OE} + W_{PL}}\right) \quad (18)$$

For a conventional powertrain, $(g/e_f) \cdot E_{0,tot}$ equals the fuel weight W_f of the aircraft and $\eta_1 \eta_3 = \eta_{gt} \eta_p$ (see Table 1), and hence the conventional Breguet range equation of Eq. (1) is obtained. The same expression is applicable to turboelectric powertrains, although in that case the additional efficiency contributions of the electrical components are included ($\eta_1 \eta_3 = \eta_{gt} \eta_{eg} \eta_{em} \eta_p$). This implies that, for the same aeropropulsive efficiency and weight breakdown, a conventional aircraft will always outperform a turboelectric variant.

B.   Fully Electrical Configurations

For fully battery-based configurations, the supplied power ratio is equal to one. However, when substituting $\Phi = 1$ in Eq. (17), an indeterminate $\infty \cdot 0$ is obtained, as expected from Eq. (4). Therefore, the limit $\Phi \to 1$ has to be analyzed. By performing a Taylor series expansion around $\Phi = 1$, the limit can be computed as

$$\lim_{\Phi \to 1} R(\Phi) = \frac{abn}{c+m} + \frac{an(2(b-1)c + bn - 2m)}{2(c+m)^2}(\Phi - 1)$$
$$+ O((\Phi - 1)^2) \quad (19)$$

where the dummy variables $a - n$ are given by

$$a = \eta_1 \eta_3 \frac{L}{D} \frac{e_f}{g} \quad (20a)$$

$$b = \frac{\eta_2}{\eta_1} \quad (20b)$$

$$c = W_{OE} + W_{PL} \quad (20c)$$

$$m = \frac{g}{e_{bat}} E_{0,tot} \quad (20d)$$

$$n = \frac{g}{e_f} E_{0,tot} \quad (20e)$$

Therefore, by neglecting higher-order terms, in the limit of $\Phi \to 1$ the range is equal to

$$R = \eta_2 \eta_3 \left(\frac{L}{D}\right) \frac{E_{0,tot}}{W_{OE} + W_{PL} + (g/e_{bat})E_{0,tot}} \quad (21)$$

Given that $\eta_2 \eta_3 = \eta_{em} \eta_p$, irrespective of the type of powertrain node considered (see Table 1), in this case the range equation of the electrical architecture [Eq. (2)] is obtained. It is interesting to note that, although Eq. (17) differs from the equations derived in Refs. [3,35,40], in the limit $\Phi \to 1$, the different approaches result in the same expression. This is because, in the case of $\Phi = 1$, the aircraft weight remains constant and thus Eq. (2) is valid for

"hybrid-electric" aircraft. Moreover, in that case, the order in which the two energy sources are used is irrelevant, because one of them contains zero energy.

V.   Demonstration

To provide an example, Fig. 3 presents the range computed using Eq. (17) as a function of the supplied power ratio Φ and battery specific energy e_{bat}. A mechanical-node powertrain (i.e., a parallel architecture; see Fig. 1a) is used in this example. The values selected for the different variables are gathered in Table 2. From Fig. 3 it is evident that the range equation provides a smooth response surface, even when the supplied power ratio tends to one. The figure shows that, at low supplied-power ratios, the range is practically independent of the battery technology level, because the powertrain approaches a conventional fuel-based powertrain. Conversely, at low specific-energy values, the range is nearly independent of the supplied power ratio. This is because, for a given total energy on-board, the battery weight increases drastically as $e_{bat} \to 0$. Thus, for $e_{bat} = 0$, $\Phi > 0$, zero range is achieved, whereas for $\Phi = 0$, the range of a conventional aircraft is achieved.

At a battery specific energy of $e_{bat} \approx 500$ Wh/kg, the range is practically independent of the supplied power ratio, and equal to the range of the fuel-based aircraft. Below this value, the range of the aircraft decreases with increasing Φ, whereas above it, the range increases with Φ. This occurs because, for high e_{bat} values, the high transmission efficiency of the electrical powertrain branch leads to an energy saving that offsets the weight penalty of the batteries. The opposite occurs at low e_{bat} values, where the high energy density of fuel compensates the lower conversion efficiency of the combustion engine. The location of the curve that divides these two regions depends on the weight breakdown of the aircraft and the transmission efficiency of the powertrain components (η_{gt}, η_{em}, and η_{eg}). For the values selected in Table 2, it is almost independent of the supplied power ratio.

Finally, Fig. 3 confirms that, for the battery specific energy values available today at pack level (100 Wh/kg < e_{bat} < 300 Wh/kg), the maximum range is achieved for $\Phi = 0$. However, a different optimum may be found for smaller aircraft, or if a different metric, such as in-flight emissions, is used to select the optimum degree-of-hybridization. Moreover, many hybrid-electric concepts (particularly turboelectric configurations) aim to increase the aeropropulsive efficiency of the aircraft. In those cases, the range equation can be combined with a preliminary sizing method such as the one described in Ref. [19] to rapidly evaluate the design space and determine how much η_p and L/D have to increase in order to provide a benefit at aircraft level.
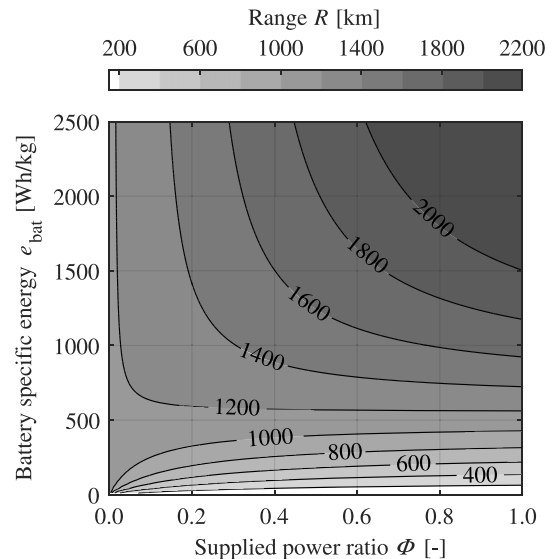
Fig. 3   Aircraft range as a function of supplied power ratio and battery specific energy.

Table 2   Values assumed for demonstration case

Variable	Value
W_{OE}, N	50,000
W_{PL}, N	20,000
$E_{0,tot}$, GJ	25
L/D	12
η_{gt}	0.35
η_{em}	0.95
η_p	0.80
e_f, Wh/kg	11,900
g, m/s^2	9.81

VI. Conclusions

In this paper, a range equation has been derived for conventional (fuel-based), fully-electric, and hybrid-electric aircraft with a constant power split. The equation is shown to be identical to the traditional Breguet range equation for the limit case of zero supplied power ratio Φ. Analogously, for fully-electric configurations ($\Phi = 1$), the equation matches the expressions found in the literature. A simple demonstration exercise shows that the equation provides a smooth response in the limits of $\Phi = 0$ and $\Phi = 1$, and that it can provide insight into the effect of battery technology level and other design considerations of hybrid-electric aircraft, without requiring detailed knowledge of the aircraft configuration. The equation can be combined with methods capable of estimating the installed power and empty weight of hybrid-electric aircraft, in order to analyze the design space or to provide initial values for more advanced design routines.

Acknowledgments

References

[1] Anon., "Realising Europe's Vision for Aviation: Strategic Research & Innovation Agenda, Vol. 1," Advisory Council for Aviation Research and Innovation in Europe, 2012.

[2] Bonet, J. T., Schellenger, H. G., Rawdon, B. K., Elmer, K. R., Wakayama, S. R., Brown, D. L., and Guo, Y., "Environmentally Responsible Aviation (ERA) Project—N+2 Advanced Vehicle Concepts Study and Conceptual Design of Subscale Test Vehicle (STV): Final Report," NASA CR-2011-216519, Dec. 2011.

[3] Geiß, I., and Voit-Nitschmann, R., "Sizing of the Energy Storage System of Hybrid-Electric Aircraft in General Aviation," CEAS Aeronautical Journal, Vol. 8, No. 1, 2017, pp. 53–65.
https://doi.org/10.1007/s13272-016-0220-5

[4] Dean, T. S., Wroblewski, G. E., and Ansell, P. J., "Mission Analysis and Component-Level Sensitivity Study of Hybrid-Electric General-Aviation Propulsion Systems," Journal of Aircraft, Vol. 55, No. 6, 2018, pp. 2454–2465.
https://doi.org/10.2514/1.C034635

[5] Kreimeier, M., and Stumpf, E., "Benefit Evaluation of Hybrid Electric Propulsion Concepts for CS-23 Aircraft," CEAS Aeronautical Journal, Vol. 8, No. 4, 2017, pp. 691–704.
https://doi.org/10.1007/s13272-017-0269-9

[6] Epstein, A. H., and O'Flarity, S. M., "Considerations for Reducing Aviation's CO$_2$ with Aircraft Electric Propulsion," Journal of Propulsion and Power, Vol. 35, No. 3, 2019, pp. 572–582.
https://doi.org/10.2514/1.B37015

[7] Gnadt, A. R., Speth, R. L., Sabnis, J. S., and Barrett, S. R. H., "Technical and Environmental Assessment of All-Electric 180-Passenger Commercial Aircraft," Progress in Aerospace Sciences, Vol. 105, Feb. 2019, pp. 1–30.
https://doi.org/10.1016/j.paerosci.2018.11.002

[8] Lents, C., Hardin, L., Rheaume, J., and Kohlman, L., "Parallel Hybrid Gas-Electric Geared Turbofan Engine Conceptual Design and Benefits Analysis," 52nd AIAA/SAE/ASEE Joint Propulsion Conference, AIAA Paper 2016-4610, July 2016.
https://doi.org/10.2514/6.2016-4610

[9] Perullo, C. A., Trawick, D. R., and Mavris, D. N., "Assessment of Engine and Vehicle Performance Using Integrated Hybrid-Electric Propulsion Models," Journal of Propulsion and Power, Vol. 32, No. 6, 2016, pp. 1305–1314.
https://doi.org/10.2514/1.B35744

[10] Gladin, J. C., Trawick, D., Mavris, D., Armstrong, M., Bevis, D., and Klein, K., "Fundamentals of Parallel Hybrid Turbofan Mission Analysis with Application to the Electrically Variable Engine," 2018 AIAA/IEEE Electric Aircraft Technologies Symposium, AIAA Paper 2018-5024, July 2018.
https://doi.org/10.2514/6.2018-5024

[11] Schmollgruber, P., Döll, C., Hermetz, J., Liaboeuf, R., Ridel, M., Cafarelli, I., Atinault, O., François, C., and Paluch, B., "Multidisciplinary Exploration of DRAGON: An ONERA Hybrid Electric Distributed Propulsion Concept," 2019 AIAA Aerospace Sciences Meeting, AIAA Paper 2019-1585, Jan. 2019.
https://doi.org/10.2514/6.2019-1585

[12] Felder, J. L., Brown, G. V., Kim, H. D., and Chu, J., "Turboelectric Distributed Propulsion in a Hybrid Wing Body Aircraft," 20th International Society for Airbreathing Engines (ISABE) Conference, ISABE Paper 2011-1340, Gothenburg, Sweden, Sept. 2011.

[13] Bijewitz, J., Seitz, A., and Hornung, M., "Power Plant Pre-Design Exploration for a Turbo-Electric Propulsive Fuselage Concept," 2018 Joint Propulsion Conference, AIAA Paper 2018-4402, July 2018.
https://doi.org/10.2514/6.2018-4402

[14] Jansen, R. H., Duffy, K. P., and Brown, G. V., "Partially Turboelectric Aircraft Drive Key Performance Parameters," 53rd AIAA/SAE/ASEE Joint Propulsion Conference, AIAA Paper 2015-3890, July 2017.
https://doi.org/10.2514/6.2015-3890

[15] Isikveren, A. T., "Method of Quadrant-Based Algorithmic Nomographs for Hybrid/Electric Aircraft Predesign," Journal of Aircraft, Vol. 55, No. 1, 2018, pp. 396–405.
https://doi.org/10.2514/1.C034355

[16] Pornet, C., Gologan, C., Vratny, P. C., Seitz, A., Schmitz, O., Isikveren, A. T., and Hornung, M., "Methodology for Sizing and Performance Assessment of Hybrid Energy Aircraft," Journal of Aircraft, Vol. 52, No. 1, 2015, pp. 341–352.
https://doi.org/10.2514/1.C032716

[17] Bryson, D. E., Marks, C. R., Miller, R. M., and Rumpfkeil, M. P., "Multidisciplinary Design Optimization of Quiet, Hybrid-Electric Small Unmanned Aerial Systems," Journal of Aircraft, Vol. 53, No. 6, 2016, pp. 1959–1963.
https://doi.org/10.2514/1.C033455

[18] Riboldi, C. E. D., "An Optimal Approach to the Preliminary Design of Small Hybrid-Electric Aircraft," Aerospace Science and Technology, Vol. 81, Oct. 2018, pp. 14–31.
https://doi.org/10.1016/j.ast.2018.07.042

[19] de Vries, R., Brown, M., and Vos, R., "Preliminary Sizing Method for Hybrid-Electric Distributed-Propulsion Aircraft," Journal of Aircraft, Vol. 56, No. 6, 2019, pp. 2172–2188.
https://doi.org/10.2514/1.C035388

[20] Finger, D. F., Braun, C., and Bil, C., "An Initial Sizing Methodology for Hybrid-Electric Light Aircraft," 2018 Aviation Technology, Integration, and Operations Conference, AIAA Paper 2018-4229, June 2018.
https://doi.org/10.2514/6.2018-4229

[21] Friedrich, C., and Robertson, P. A., "Hybrid-Electric Propulsion for Aircraft," Journal of Aircraft, Vol. 52, No. 1, 2015, pp. 176–189.
https://doi.org/10.2514/1.C032660

[22] Voskuijl, M., van Bogaert, J., and Rao, A. G., "Analysis and Design of Hybrid Electric Regional Turboprop Aircraft," CEAS Aeronautical Journal, Vol. 9, No. 1, 2018, pp. 15–25.
https://doi.org/10.1007/s13272-017-0272-1

[23] Wroblewski, G. E., and Ansell, P. J., "Mission Analysis and Emissions for Conventional and Hybrid-Electric Commercial Transport Aircraft," Journal of Aircraft, Vol. 56, No. 3, 2019, pp. 1200–1213.
https://doi.org/10.2514/1.C035070

[24] Hoelzen, J., Liu, Y., Bensmann, B., Winnefeld, C., Elham, A., Friedrichs, J., and Hanke-Rauschenbach, R., "Conceptual Design of Operation Strategies for Hybrid-Electric Aircraft," Energies, Vol. 11, No. 1, 2018, p. 217.
https://doi.org/10.3390/en11010217

[25] Roskam, J., Airplane Design, DARcorporation, Lawrence, KS, 1985, Part 1, Chap. 2.

[26] Raymer, D. P., Aircraft Design: A Conceptual Approach, AIAA Education Series, AIAA, Reston, VA, 2002, Chap. 3.
https://doi.org/10.2514/4.869112

[27] Torenbeek, E., *Synthesis of Subsonic Airplane Design*, Delft University Press, Delft, the Netherlands, 1982, Chap. 5.

[28] Hepperle, M., "Electric Flight—Potential and Limitations," NATO Rept. STO-MP-AVT-209, 2012.

[29] Traub, L. W., "Range and Endurance Estimates for Battery-Powered Aircraft," *Journal of Aircraft*, Vol. 48, No. 2, 2011, pp. 703–707.
https://doi.org/10.2514/1.C031027

[30] Avanzini, G., and Giulietti, F., "Maximum Range for Battery-Powered Aircraft," *Journal of Aircraft*, Vol. 50, No. 1, 2013, pp. 304–307.
https://doi.org/10.2514/1.C031748

[31] Patterson, M. D., German, B. J., and Moore, M. D., "Performance Analysis and Design of On-Demand Electric Aircraft Concepts," *12th AIAA Aviation Technology, Integration, and Operations Conference*, AIAA Paper 2012-5474, Sept. 2012.
https://doi.org/10.2514/6.2012-5474

[32] Sliwinski, J., Gardi, A., Marino, M., and Sabatini, R., "Hybrid-Electric Propulsion Integration in Unmanned Aircraft," *Energy*, Vol. 140, Dec. 2017, pp. 1407–1416.
https://doi.org/10.1016/j.energy.2017.05.183

[33] Kuhn, H., Falter, C., and Sizmann, A., "Renewable Energy Perspectives for Aviation," *Proceedings of the 3rd CEAS Air & Space Conference and 21st AIDAA Congress*, Council of European Aerospace Societies, Brussels, Belgium, 2011, pp. 24–28.

[34] Brelje, B. J., and Martins, J. R. R. A., "Electric, Hybrid, and Turbo-electric Fixed-Wing Aircraft: A Review of Concepts, Models, and Design Approaches," *Progress in Aerospace Sciences*, Vol. 104, Jan. 2019, pp. 1–19.
https://doi.org/10.1016/j.paerosci.2018.06.004

[35] Marwa, M., Martin, S. M., Martos, B. C., and Anderson, R. P., "Analytic and Numeric Forms for the Performance of Propeller-Powered Electric and Hybrid Aircraft," *55th AIAA Aerospace Sciences Meeting*, AIAA Paper 2017-0211, Jan. 2017.
https://doi.org/10.2514/6.2017-0211

[36] Hartmann, J., Strack, M., and Nagel, B., "Conceptual Assessment of Different Hybrid Electric Air Vehicle Options for a Commuter with 19 Passengers," *2018 AIAA Aerospace Sciences Meeting*, AIAA Paper 2018-2025, Jan. 2018.
https://doi.org/10.2514/6.2018-2025

[37] Nam, T., "A Generalized Sizing Method for Revolutionary Concepts under Probabilistic Design Constraints," Ph.D. Dissertation, Georgia Inst. of Technology, Atlanta, GA, 2007.

[38] Ravishankar, R., and Chakravarthy, S. R., "Range Equation for a Series Hybrid-Electric Aircraft," *2018 Aviation Technology, Integration, and Operations Conference*, AIAA Paper 2018-3208, June 2018.
https://doi.org/10.2514/6.2018-3208

[39] Rohacs, J., and Rohacs, D., "Energy Coefficients for Comparison of Aircraft Supported by Different Propulsion Systems," *Energy*, Vol. 191, Jan. 2019, Paper 116391.
https://doi.org/10.1016/j.energy.2019.116391

[40] Elmousadik, S., Ridard, V., Sécrieru, N., Joksimovic, A., Maury, C., and Carbonneau, X., "New Preliminary Sizing Methodology for a Commuter Airplane with Hybrid-Electric Distributed Propulsion," *Advanced Aircraft Efficiency in a Global Air Transport System (AEGATS 18)*, Association Aéronautique et Astronautique de France Paper AEGATS2018-50, Toulouse, France, Oct. 2018.

[41] Perullo, C., and Mavris, D., "A Review of Hybrid-Electric Energy Management and Its Inclusion in Vehicle Sizing," *Aircraft Engineering and Aerospace Technology: An International Journal*, Vol. 86, No. 6, 2014, pp. 550–557.
https://doi.org/10.1108/AEAT-04-2014-0041

[42] National Academies of Sciences, Engineering, and Medicine, *Commercial Aircraft Propulsion and Energy Systems Research: Reducing Global Carbon Emissions*, National Academies Press, Washington, D.C., 2016, Chap. 4.
https://doi.org/10.17226/23490

[43] Isikveren, A. T., Kaiser, S., Pornet, C., and Vratny, P. C., "Pre-Design Strategies and Sizing Techniques for Dual-Energy Aircraft," *Aircraft Engineering and Aerospace Technology: An International Journal*, Vol. 86, No. 6, 2014, pp. 525–542.
https://doi.org/10.1108/AEAT-08-2014-0122

[44] Isikveren, A. T., Pornet, C., Vratny, P. C., and Schmidt, M., "Optimization of Commercial Aircraft Using Battery-Based Voltaic-Joule/Brayton Propulsion," *Journal of Aircraft*, Vol. 54, No. 1, 2017, pp. 246–261.
https://doi.org/10.2514/1.C033885

[45] Pornet, C., and Isikveren, A. T., "Conceptual Design of Hybrid-Electric Transport Aircraft," *Progress in Aerospace Sciences*, Vol. 79, Nov. 2015, pp. 114–135.
https://doi.org/10.1016/j.paerosci.2015.09.002